Synthesis, characterization and antibiotic evaluation of some novel (*E*)-3-(4-diphenylamino) phenyl)-1-(4′-fluorophenyl)prop-2-en-1-one chalcones and their analogues

AbdulRazaq Tukur*, James Dama Habila, Rachael Gbekele-Oluwa Ayo and Ogunkemi Risikat Agbeke Iyun

Abstract

Background: The increase in resistance of pathogenic organisms to the available chemotherapeutic agents are critical challenges in drug design and development, motivating researchers to look for novel compounds that can combat multidrug-resistant organisms. Recently, chalcones have been proved to be attractive moieties in drug discovery.

Results: Eight novel triphenylamine chalcones with different substitution patterns were successfully synthesized via the conventional Claisen–Schmidt condensation reaction in an alkaline medium at room temperature, and recrystallized using ethanol, the percentage yield of the compounds were between 30 and 92%. The structures of the synthesized chalcones were successfully characterized and confirmed using FT-IR, NMR spectroscopic and GC–MS spectrometric techniques.

Conclusions: The results of the biological studies showed that all the synthesized chalcones possess remarkable activities against the tested microbes, by showing a significant zone of inhibitions relative to that of the standard drugs used. The investigation revealed that *1b* showed highest ZOI (30 mm), lowest MIC (12.5 μg/ml) and MBC/MFC (50 μg/ml) on *Aspergillus niger*. Therefore, displayed better antifungal potential as compared to the rest of the compounds, and can be a potential antifungal drug candidate.

Keywords: Acetophenone, Antibiotics, Condensation, Recrystallization, Propiophenone

1 Background

Synthesis and biodynamic activities of chalcones have attracted people's attention recently. Chalcone has an exceptional synthon, enabling the development of a diverse variety of novel heterocycles with interesting pharmacological characteristics [39]. Due to a wide range of structural modifications, chalcones have shown promising therapeutic efficacy, and had been applied in the cure several infections [20]. In fact, few structurally varied compounds display connection with such a broad range of pharmacological actions. Chalcone and its derivatives show varied range of outstanding biological properties, such as anti-tumor [1, 35], antifungal [8], antiviral [38], anti-inflammatory [2–5], anticancer [7, 10, 11], antibacterial [12–14], antidiabetic [15, 17, 34], and antioxidant [18, 19, 28, 40] and antihypertensive activities [6, 21]. The synthesis of chalcones and derivative has continued to attract much interest in synthetic organic chemistry [22, 36].

*Correspondence: abdulrazaqtukur@gmail.com

Department of Chemistry, Ahmadu Bello University, Zaria, Kaduna State, Nigeria

Tukur *et al. Beni-Suef Univ J Basic Appl Sci* (2022) 11:66

Page 2 of 11

Chalcones have been prepared using various methods, but the most typical is the Claisen–Schmidt condensation in an acidic or basic medium, under homogeneous circumstances [23, 25–27]. This study aimed to synthesize, characterize and investigate the biological potentials of some (*E*)-3-(4-diphenylamino)phenyl)-1-(4′-fluorophenyl)prop-2-en-1-one chalcones and their analogues.

2 Methods

2.1 General procedure for the synthesis of (1a–d and 2a–d)

To a 100 mL round bottomed flask, equipped with a magnetic stirrer, dissolved in 25 mL ethanol, equimolar quantities of 4-(diphenylamino)benzaldehyde (0.4 g, 1.5 mmol) and substituted acetophenones/propiophenone (0.4 g, 2 mmol) were transferred and stirred for 30 min. A solution of sodium hydroxide (10 mL, 10%) was added dropwise while stirring. The reaction temperature was maintained between 20 and 24 °C for 4–5 h. A thin layer chromatographic method was used to examine the progress and completion of the reaction. The reaction mixture was refrigerated for 10 h after completion. Formation of precipitate was observed, which was filtered, rinsed numerous times with water (100 ml), dried in the open air and purified using recrystallization method from ethanol (30 ml) to obtained a triphenylamine chalcone, (**1a**–**d**, **2a**–**d**) Hongtian et al., [24]. Table 2 shows the confirmed structures of the synthesized triphenylamine chalcones and their percentage yields.

2.2 Spectral analysis

FTIR spectroscopy is the technique used to identify the functional groups in a compound. The samples were scanned in a range of 650 to 4000 cm^{-1}. KBr disk method was used to record the IR spectra of the solid product using a PerkinElmer Spectrum 100 FTIR spectrometer. A GC 7890B, MSD 5977A, Agilent Tech and mass detector were used to analyze the synthesized chalcones. At a flow rate of 1 mL/min, helium was used as the carrier gas, and 1L of the sample supernatant was fed into the GC. The GC oven temperature was programmed to rise from 80 °C to 200 °C at a rate of 15 °C/min, then to 280 °C at a rate of 5 °C/min, with a 5-min isothermal at 280 °C. The temperature of the ion source was set to 230 °C, and the ionization voltage was set to 70 eV. The National Institute of Standards and Technology's database was used for GC–MS interpretation (NIST). The mass spectrum of the synthesized chalcones was compared with the spectrum of the known components stored in the NIST library. To confirm the structures of the synthesized chalcones, NMR (^{1}H and ^{13}C) investigations were performed. ^{1}H and ^{13}C-NMR spectra were obtained on a Bruker Advance III400 MHz Spectrometer at room temperature,

(400 MHz for both ^{1}H and ^{13}C), using the TMS as reference. Chemical shift values (δ) were reported in parts per million (ppm) relative to TMS standard, and coupling constant (J) are given in Hz. For these tests, deuterated chloroform was used as the solvent (CDCl$_3$-d6). Before being transferred into an NMR tube, about 20 mg of sample was dissolved in deuterated solvent. The following are the several types of multiplicities: singlet (s), doublet (d), doublet of doublets (dd), triplet (t), quartet (q) and multiplet (m).

2.3 Biological studies

Generally chalcones have shown remarkable pharmacological applications, the antimicrobial potentials of the synthesized compounds were tested against some selected gram positive and gram negative bacteria and fungi collected from the Department of Pharmaceutical Microbiology, Faculty of Pharmaceutical Sciences, Ahmadu Bello University, Zaria, Nigeria. These include; *- Escherichia coli, Pseudomonas aeruginosa, Salmonella typhi, Staphylococus aureus, Bacillus substilis, Candida albicans, Aspergillus niger* and Methicilin Resistant *Staphylococus aureus* (MRSA). These organisms were selected.

2.3.1 Determination of zone of inhibition (ZOI)

The compounds (0.005 mg) were weighed and dissolved in 10 mL dimethyl sulfoxide (DMSO) to obtain a concentration of 50 μg/mL, this was the initial concentration used to determine the microbial successibility of the compounds. Mueller–Hinton agar was the medium used as the growth medium for the test. The medium was prepared according to the manufacturer's instructions, sterilized at 121 °C for 15 min, poured into sterile petri dishes and was left to cool and solidify. Diffusion method was used for screening the extracts. The sterilized medium was seeded with 0.1 mL of the standard inoculum of the test microbes; the inoculum was spread evenly over the surface of the medium using a sterile swab. The solution of the compounds (0.1 mL) of 50 μg/mL was the then introduced into each well on the inoculated medium. Incubation was made at 37 °C for 24 h for bacteria and 48 h for fungi, after which each plate of the medium was observed for zone of inhibition of growth. The zone was measured with a pair of divider and a ruler and the result recorded in millimeters (mm) [29].

2.3.2 Determination of minimum inhibitory concentration (MIC)

The minimum inhibitory concentrations (MIC) of the synthesized compounds were determined by using the broth dilution method as reported by Bruton et al. [9]. Mueller–Hinton Broth (MHB) was prepared according

Tukur *et al. Beni-Suef Univ J Basic Appl Sci*   (2022) 11:66

Page 3 of 11

to manufacturer's instructions, 10 mL was dispensed into test tubes and the broth was sterilized at 121 °C for 15 min, the broth was allowed to cool. Mc-Farland's turbidity standard scale number 0.5 was prepared to obtain a turbid solution. Normal saline was also prepared, 10 mL was dispensed into sterilized test tubes, and the test microbes were inoculated and incubated at 37 °C for 6 h. Dilution of the test microbes was done in the normal saline until the turbidity marched that of the Mc-Farland's scale by visual comparison, at this point the test microbes has a concentration of about 1.5×10^8 CFU/mL. Twofold serial dilution of the test compounds in the sterile broth was made to obtain the concentrations of 100 µg/mL, 50 µg/mL, 25 µg/mL, 12.5 µg/mL, 6.25 µg/mL and 3.125 µg/mL, respectively. Having obtained the different concentrations of the compounds in the sterile broth, 0.1 mL of the test microbes in the normal saline was then introduced (inoculated) into the different concentrations, and incubated at 37 °C for 24 h, after which each test tube was observed for turbidity (growth), the lowest concentration of the compounds in the broth which shows no turbidity was recorded as the minimum inhibitory concentration [9].
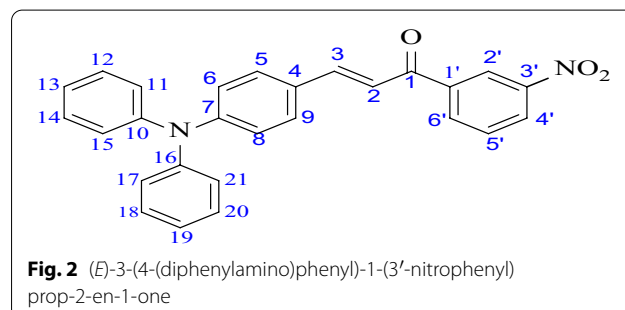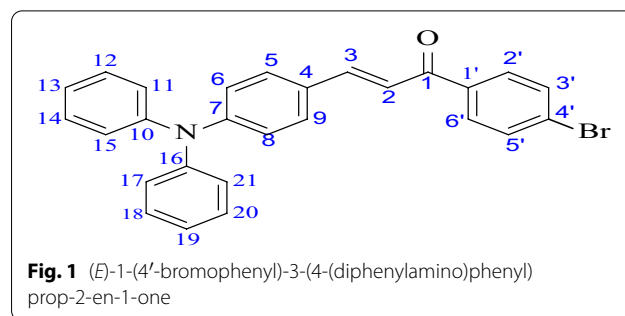
2.3.3 Determination of minimum bactericidal/fungicidal concentration (MBC/MFC)

The MBC/MFC were carried out to determine whether the test microbes were killed. Mueller–Hinton agar was prepared, sterilized at 121 °C for 45 min, poured into sterile petri dishes and allowed to cool and solidify. The content of the MIC in the serial dilution was then subcultured onto prepared medium, incubation was made at 37 °C for 24 h for bacteria and 48 h for fungi, after which the plates were observed for colony growth, the MBC/MFC were the plates with lowest concentration of the test compounds without colony growth [9].

3 Results

3.1 Result of spectroscopic analyses

(*E*)-1-(4′-bromophenyl)-3-(4-(diphenylamino)phenyl)prop-2-en-1-one (1a) was obtained as deep yellow solid powder at 70% yield. Its melting point was determined to be 145–147 °C. The IR spectrum (Additional file 1: Appendix 1) showed the following prominent peaks (cm^{-1}); 3041 (=C–H), 1684 (C=O), 1580 (C=C), 1267 (C–N) and 530 (C–Br). The GC–MS analysis showed the molecular ion peak of 454 m/z (Additional file 1: Appendix 2). The NMR spectral showed the following signals; ^{1}H-NMR (400 MHz, CDCl$_3$) δ 8.03 (d, 1H $J=15.3$ Hz, 3-H), 7.68 (d, 2H, $J=3.0$ Hz, 2′,6′-H), 7.57 (d, 1H, $J=12.1$ Hz, 2-H), 7.43 (d, 2H, $J=4.4$ Hz, 3′,5′-H), 7.38 (d, 2H, $J=7.8$ Hz, 5,9-H), 7.35 (d, 2H, $J=6.5$–2.1 Hz, 11,15,17, 21-H), 7.18

Fig. 1 (*E*)-1-(4′-bromophenyl)-3-(4-(diphenylamino)phenyl) prop-2-en-1-one

Fig. 2 (*E*)-3-(4-(diphenylamino)phenyl)-1-(3′-nitrophenyl) prop-2-en-1-one

(d, 2H, $J=5.4$–1.8 Hz, 12,14,18,20-H) 7.08 (d, 2H, $J=3.2$–28 Hz,13,19-H) and 7.02 (d, 2H, $J=8.7$ Hz, 6,8-H) (Additional file 1: Appendix 3), ^{13}C-NMR (400 MHz, CDCl$_3$) δ 190.29 (C-1), 149.68 (C-3,7), 145.95 (C-10,16), 130.73 (C-3′–5′), 130 (C-2′,6′), 129.90 (C-4,12,14,18,20), 128.51 (C-13,19), 126.02 (C-11,15,17,21), 125 (C-4′), 124 (C-6,8) and 119.29 (C-2) (Additional file 1: Appendix 4) (Fig. 1).

(*E*)-3-(4-(diphenylamino)phenyl)-1-(3′-nitrophenyl) prop-2-en-1-one (1b) was obtained as golden yellow solid powder at 92% yield. Its melting point was found to be 143–145 °C. The IR spectrum (Additional file 1: Appendix 5) showed the following prominent peaks (cm^{-1}); 3037 (=C–H), 1684 (C=O), 1580 (C=C), 1390 (N=O) and 1285 (C–N). The GC–MS analysis showed the molecular ion peak of 420 m/z (Additional file 1: Appendix 6). The NMR spectral showed the following signals; ^{1}H-NMR (400 MHz, CDCl$_3$) δ 8.75 (s, 1H, 2′-H), 8.47 (d, $J=3.3$ Hz, 4′-H), 8.26 (d, 1H, $J=4.3$ Hz, 6′-H), 8.13 (d, 1H, $J=14.6$ Hz, 2H), 8.02 (t, 1H, $J=5.6$ Hz, 5′-H), 7.97 (d, 1H, $J=12.3$ Hz, 3-H), 7.79 (d, 2H, $J=8.7$ Hz, 6,8-H) and 7.60 (d, 2H, $J=3.2$ Hz, 5,9-H), 7.18 (d, 2H, $J=5.4$ 2.4 Hz, 11,15,17,21-H), 7.13 (d, 2H, $J=6.4$–2.8 Hz, 12,14,18,20-H) and 7.02 () (Additional file 1: Appendix 7), ^{13}C-NMR (400 MHz, CDCl$_3$) δ 190.46 (C-1), 149.23 (C-3′), 145.9 (C-10,16), 144.6 (C-7), 142.8 (C-3), 138.87 (C-1′), 133.82 (C-6′), 131.29 (C-5′), 129.73 (C-4′), 129.7 (C-5,9), 129.6 (C-12,14,18,20), 126.9 (C-13,19), 126.29 (C-6,8), 125.7 (C-11,15,17,21), 125.08 (C-4), 123.29 (C-2′) and 119.08 (C-2) (Additional file 1: Appendix 8) (Fig. 2).
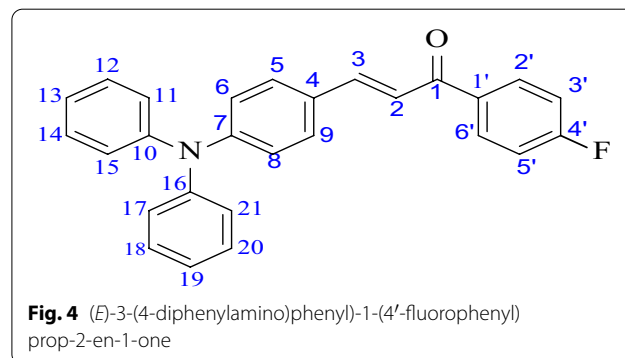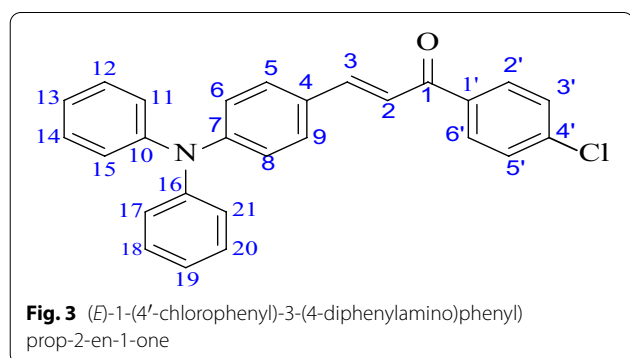
Tukur *et al. Beni-Suef Univ J Basic Appl Sci*   (2022) 11:66

Page 4 of 11

(*E*)-1-(4′-chlorophenyl)-3-(4-diphenylamino)phenyl)prop-2-en-1-one (1c) was obtained as yellow solid powder at 57% yield. Its melting point was determined to be 137–139 °C. The IR spectrum (Additional file 1: Appendix 9) showed the following prominent peaks (cm^{-1}); 3036 (=C–H), 1684 (C=O), 1580 (C=C), 1285 (C–N) and 620 (C–Cl). The GC–MS analysis showed the molecular ion peak of 409 m/z (Additional file 1: Appendix 10). The NMR spectral showed the following signals; ^{1}H-NMR (400 MHz, CDCl$_3$) δ 8.51 (d, 1H, $J=13.3$ Hz, 3-H), 8.15 (d, 2H, $J=4.3$ Hz, 2′,6′-H), 7.68 (d, 1H, $J=12.5$ Hz, 2-H), 7.46 (d, 2H, $J=8.4$ Hz, 3′,5′-H), 7.33 (d, 2H, $J=2.7$ Hz, 6,8-H) 7.22 (d, 2H, $J=7.3$–3.4 Hz, 12,14,18,20-H) 7.17 (d, 2H, $J=2.7$ Hz, 5, 9-H), 7.15 (d, 2H, $J=3.3$–1.8 Hz, 11,14,17,21-H) and 6.97 (d, 2H, $J=4.3$–2.1 Hz, 13,19-H) (Additional file 1: Appendix 11). ^{13}C-NMR (400 MHz, CDCl$_3$) δ 190.46 (C-1), 149.48 (C-3,7), 145.88 (C-10,16), 142.74 (C-4′), 136.50 (C-1′), 131.30 (C-3′,5′), 129.70 (C-2′,6′,5,9), 129.60 (C-12,14,18,20), 128.40 (C-4), 126.8 (C-13,19), 126.29 (C-6,8), 125.09 (C-11,15,17,21) and 119.30 (C-2) (Additional file 1: Appendix 12) (Fig. 3).
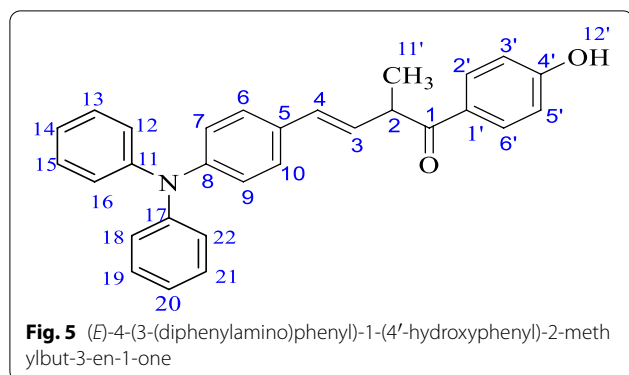
(*E*)-3-(4-diphenylamino)phenyl)-1-(4′-fluorophenyl)prop-2-en-1-one (1d) was obtained as lemon green solid powder at 60% yield. Its melting point was found to be 136–138 °C. The IR spectrum (Additional file 1: Appendix 13) showed the following prominent peaks (cm^{-1}); 3037 (=C–H), 1684 (C=O), 1580 (C=C), 1286 (C–N) and 1073 (C–F). The GC–MS analysis showed the molecular ion peak of 393 m/z (Additional file 1: Appendix 14). The NMR spectral showed the following signals; ^{1}H-NMR (400 MHz, CDCl$_3$) δ 8.44 (d, 1H, $J=12.8$ Hz, 3-H), 8.29 (d, 2H, $J=7.8$ Hz, 2′, 6′-H), 7.68 (d, 1H, $J=11.3$ Hz, 2-H), 7.42 (d, 2H, $J=6.3$–3.1 Hz, 12,14,18,20-H), 7.35 (d, 2H, $J=6.2$ Hz, 3′,5′-H), 7.16 (d, 2H, $J=5.0$ Hz, 5,9-H), 7.15 (d, 2H, $J=7.0$ Hz, 6,8-H), 7.09 (d, 2H, $J=4.5$–1.2 Hz, 11,15,17,21-H) and 6.98 (d, 2H, $J=3.6$–1.2, 13,19-H) (Additional file 1: Appendix 15), ^{13}C-NMR (400 MHz, CDCl$_3$) δ 190.49 (C-1), 168.14 (C-4′), 149.7 (C-10,16), 146.10 (C-3,7), 136.36 (C-1′), 131.28 (C-2′,6′), 129.69 (C-5,9), 129.6 (C-4), 128.37 (C-12,14,18,20), 126.28 (C-13,19), 125.08 (C-11,15,17,21), 120.08 (C-6,8), 119.29 (C-2), and 116 (C-3′,5′) (Additional file 1: Appendix 16) (Fig. 4).

(*E*)-4-(3-(diphenylamino)phenyl)-1-(4′-hydroxyphenyl)-2-methylbut-3-en-1-one (2a) was obtained as pale yellow solid powder at 55% yield. Its melting point was determined to be 146–148 °C. The IR spectrum (Additional file 1: Appendix 17) showed the following prominent peaks (cm-^{1}); 3243 (O–H), 3037 (=C–H), 1684 (C=O), 1580 (C=C), 1282 (C–N). The GC–MS analysis showed the molecular ion peak of 419 m/z (Additional file 1: Appendix 18). The NMR spectral showed the following signals; ^{1}H-NMR (400 MHz, CDCl$_3$) δ 9.80 (s, 1H, 12-H), 7.96 (d, 2H, $J=6.5$ Hz, 2′,6′-H), 7.68 (d, 2H, $J=4.4$ Hz, 6,10-H), 7.32 (d, 2H, $J=8.6$ Hz, 7,9-H), 7.14 (d, 2H, $J=7.2$–1.2 Hz, 12,16,18,22-H), 7.08 (d, 2H, $J=4.3$–1.2 Hz, 13,15,19,21-H), 7.02 (d, 2H, $J=3.8$–1.3 Hz, 14,20-H), 6.63 (d, 2H, $J=11.2$ Hz, 3′,5′-H), 6.58 (d, 1H, $J=14.3$ Hz, 4-H), 6.31 (d, 1H, $J=12.7$ Hz, 3-H), 3.81 (dd,1H, $J=15.0, 7.5$ Hz, 2-H) and 0.90 (d, 3H, $J=12.3$ Hz, 11′-H) (Additional file 1: Appendix 19). ^{13}C-NMR (400 MHz, CDCl$_3$) δ 190.44 (C-1), 162.92 (C-4′), 145.1 (C-8), 145.9 (11,17), 132.66 (C-2′,6′), 131.32 (C-5), 129.8 (C-14,20), 129.45 (C-4,6,10,13,19,21), 125.94 (C-12,16,18,22), 123.2 (C-7,9), 124.30 (C-1′), 118.92 (C-3), 114.43 (C-3′,5′), 47.10 (C-2) and 17.73 C-(11′) (Additional file 1: Appendix 20) (Fig. 5).
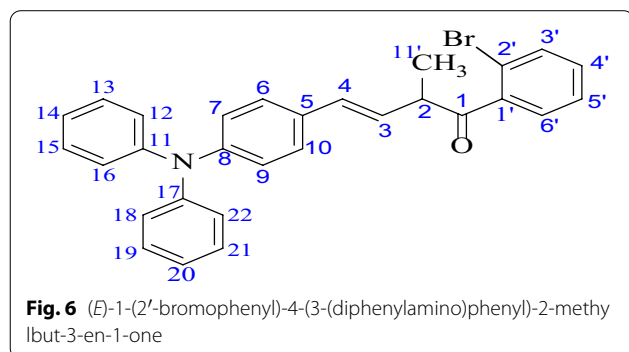
(*E*)-1-(2′-bromophenyl)-4-(3-(diphenylamino)phenyl)-2-methylbut-3-en-1-one (2b) was obtained as brownish yellow solid powder at 30% yield. Its melting point was found to be 147–148 °C. The IR spectrum (Additional file 1: Appendix 21) showed the following prominent peaks (cm^{-1}); 3037 (=C–H), 1684 (C=O), 1580 (C=C) 1285 (C–N) and 580 (C–Br). The GC–MS analysis showed the molecular ion peak of 482 m/z (Additional file 1: Appendix 22). The NMR spectral showed the following signals; ^{1}H-NMR (400 MHz, CDCl$_3$) δ 7.92
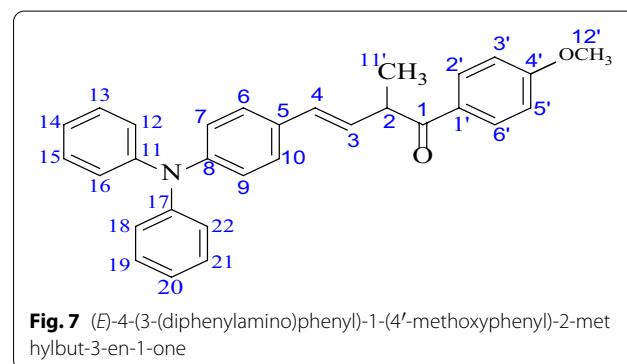

Fig. 3 (*E*)-1-(4′-chlorophenyl)-3-(4-diphenylamino)phenyl) prop-2-en-1-one

Fig. 4 (*E*)-3-(4-diphenylamino)phenyl)-1-(4′-fluorophenyl) prop-2-en-1-one

Tukur *et al. Beni-Suef Univ J Basic Appl Sci* (2022) 11:66

Page 5 of 11

Fig. 5 (*E*)-4-(3-(diphenylamino)phenyl)-1-(4′-hydroxyphenyl)-2-methylbut-3-en-1-one

(d, 1H, *J* = 9.5 Hz, 6′-H), 7.81 (d, 2H, *J* = 5.7 Hz, 6,10-H), 7.42 (d, 1H, *J* = 8.9 Hz, 3′-H), 7.39 (t, 1H, *J* = 12.4 Hz, 5′-H), 7.32 (t, 1H, *J* = 12.4 Hz, 4′-H), 7.24 (d, 2H, *J* = 9.6–5.7 Hz, 13,15,21,19-H), 7.16 (d, 2H, *J* = 10.3 Hz, 7,9-H), 7.08 (d, 2H, *J* = 10.3–7.4 Hz, 12,16,18,22-H), 6.60 (d, 1H, *J* = 15.4 Hz, 4-H), 7.0 (d, 2H, *J* = 6.3–4.1 Hz, 14,20-H), 6.33 (d, 1H, *J* = 14.0 Hz, 3-H), 3.75 (q, 1H, *J* = 30.2, 12.1 Hz, 2-H) and 0.89 (d, 3H, *J* = 15.6 Hz, 11′H) (Additional file 1: Appendix 23). ^{13}C-NMR (400 MHz, CDCl$_3$) δ 190.47 (C-1), 146.81 (C-11,17), 146.07 (C-8), 140.99 (C-1′), 133.62 (C-3′), 132.70 (C-4′), 131.29 (C-5), 129.7 (C-4,6,10), 129.69 (C-13,15,19,21), 126.8 (C-14,20), 126.29 (C-6′), 125.7 (C-12,16,18,22), 125.2 (C-5′), 125.09 (C-7,9), 119.30 (C-2′), 116 (C-3), 46.46 (C-2) and 17.59 (C-11′) (Additional file 1: Appendix 24) (Fig. 6).
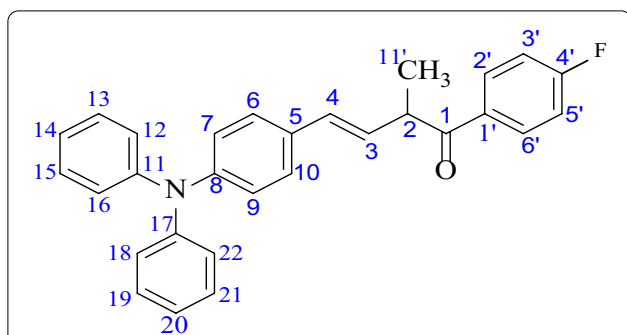
(*E*)-4-(3-(diphenylamino)phenyl)-1-(4′-methoxyphenyl)-2-methylbut-3-en-1-one (2c) was obtained as orange yellow solid powder at 52% yield. Its melting point was determined to be 142–144 °C. The IR spectrum (Additional file 1: Appendix 25) showed the following prominent peaks (cm^{-1}); 3037 (=C–H), 1684 (C=O), 1580 (C=C), 1320 (C–O) and 1285 (C–N). The GC–MS analysis showed the molecular ion peak of 433 m/z (Additional file 1: Appendix 26). The NMR spectral showed the following signals; ^{1}H-NMR (400 MHz, CDCl$_3$) δ 8.00 (d, 2H, *J* = 13.2 Hz, 2′,6′-H), 7.73 (d, 2H *J* = 13.2 Hz, 6,10-H), 7.24 (d, 2H, *J* = 9.8–3.6 Hz, 13,15,21,19-H), 7.18 (d, 2H, *J* = 14.0 Hz, 3′,5′-H), 7.13 (d, 2H, *J* = 7.3–1.3 Hz, 7,9-H), 7.08 (d, 2H, *J* = 12.5–7.6 Hz, 12,16,18,22-H), 7.00 (d, 1H, *J* = 12.6 Hz, 4-H), 6.98 (d, 2H, *J* = 6.3–3.2 Hz, 14,20-H), 6.30 (d, 1H, *J* = 11.5 Hz, 3-H), 3.90 (s, 3H, 12′-H), 3.70 (q, 1H, *J* = 13.32, 15.23 Hz, 2-H) and 0.87 (d, 3H *J* = 6.8 Hz, 11′-H) (Additional file 1: Appendix 27). ^{13}C-NMR (400 MHz, CDCl$_3$) δ 190.64 (C-1), 165.20 (C-4′), 145.8 (C-11,17), 145.1 (C-8), 131.23 (C-5), 129.7 (C-4,6,10), 129.6 (C-13,15,21,19), 129.28 (C-2′,6′), 127 (C-1′), 126.8 (C-14,20), 126.46 (C-), 125.7 (C-12,16,18,22), 124.52 (C-7,9), 115.99 (C-3), 113.4 (C-3′,5′), 55.29 (12′), 47.04 (C-2) and 17.80 (C-11′) (Additional file 1: Appendix 28) (Fig. 7).

(*E*)-4-(3-(diphenylamino)phenyl)-1-(4-fluorophenyl)-2-methylbut-3-en-1-one (2d) was obtained as cotton brown solid powder at 54% yield. Its melting point was found to be 146–148 °C. The IR spectrum (Additional file 1: Appendix 29) showed the following prominent peaks (cm^{-1}); 3037 (=C–H), 1684 (C=O), 1580 (C=C), 1287 (C–N) and 1028 (C–F). The GC–MS analysis showed the molecular ion peak of 421 m/z (Additional file 1: Appendix 30). The NMR spectral showed the following signals; ^{1}H-NMR (400 MHz, cdcl$_3$) δ 8.23 (d, 2H, *J* = 6.5 Hz, 2′,6′-H), 7.70 (d, 2H, *J* = 13.6 Hz, 6,10-H), 7.37 (d, 2H, *J* = 13.7 Hz, 3′,5′-H), 7.24 (d, 2H, *J* = 8.5–3.6 Hz, 13,15,21,19-H), 7.14 (d, 2H, *J* = 6.2–3.2 Hz, 7,9-H), 7.08 (d, 2H, *J* = 12.5–7.6 Hz, 12,16,18,22-H), 6.8 (d, 2H, *J* = 3.6–3.2 Hz, 14,20-H), 6.60 (d, 1H, *J* = 13.2 Hz, 4-H), 6.31 (d, 1H, *J* = 12.7 Hz, 3-H), 3.71 (q, 1H, *J* = 13.1, 6.7 Hz, 2-H) and 0.85 (d, 1H, *J* = 6.7 Hz, 11′-H) (Additional file 1: Appendix 31). ^{13}C-NMR (400 MHz, CDCl$_3$) δ 190.37 (C-1), 168.01 (C-4′), 146.8 (C-11,17), 146.4 (C-8), 133.89 (C-5), 131.29 (C-1′), 129.75 (C-2′,6′), 126.6 (C-13,15,19,21), 129.18 (C-4,6,10) 126.09 (C-14,20), 125.2 (C-12,16,18,22), 123.37 (C-7,9), 119.07 (C-3), 114.48 (C-3′,5′), 48.06 (C-2) and 17.74 (C-11′) (Additional file 1: Appendix 32) (Fig. 8).

Fig. 6 (*E*)-1-(2′-bromophenyl)-4-(3-(diphenylamino)phenyl)-2-methylbut-3-en-1-one

Fig. 7 (*E*)-4-(3-(diphenylamino)phenyl)-1-(4′-methoxyphenyl)-2-methylbut-3-en-1-one

Tukur *et al. Beni-Suef Univ J Basic Appl Sci*   (2022) 11:66

Page 6 of 11

Fig. 8 (*E*)-4-(3-(diphenylamino)phenyl)-1-(4-fluorophenyl)-2-methyl but-3-en-1-one

3.2 Results of the biological studies
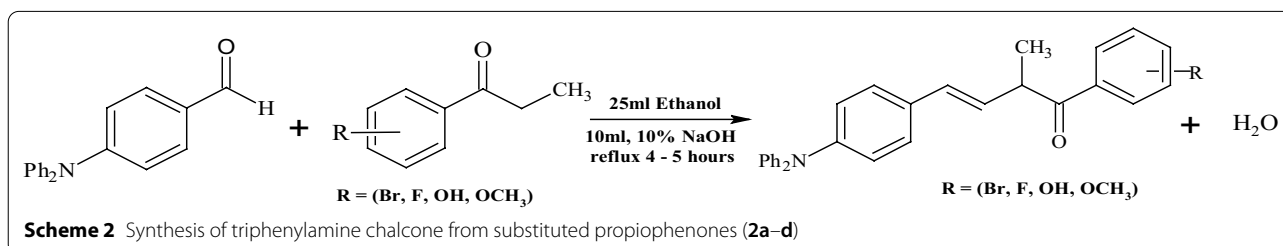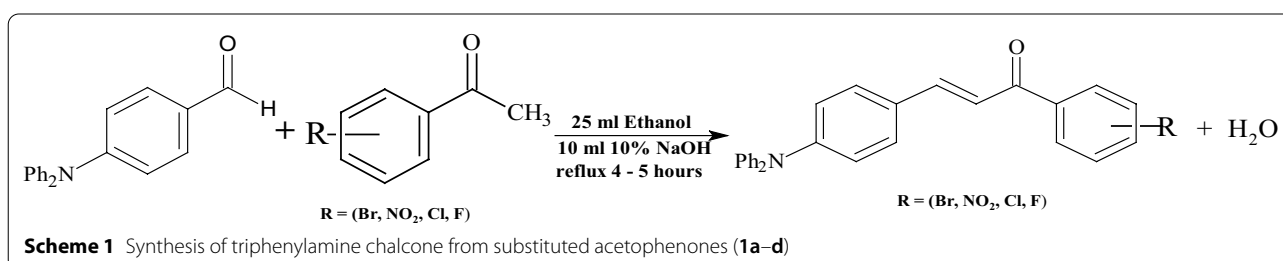See Tables 2, 3 and 4.

4 Discussion
The target triphenylamine chalcones were prepared using the Claisen–Schmidt condensation process of various substituted acetophenone/propiophenones and 4-(Diphenylamino) benzaldehyde, in the presence of NaOH (10%) in ethanol. The nucleophilic enolate attack on the electrophilic carbonyl carbon of 4-(Diphenylamino) benzaldehyde resulted in the formation of a new carbon–carbon bond, which was initiated by the removal of a proton from the α-carbon of the acetophenone/propiophenones to form a resonance-stabilized enolate ion. As a result, the α-carbon of acetophenone/propiophenones was linked to the carbonyl carbon of 4-(Diphenylamino) benzaldehyde to form an intermediate, which was then protonated and deprotonated by

hydroxide ion to form α,β-unsaturated triphenylamine chalcone.

4.1 Spectroscopic characterization of the synthesized triphenylamine chalcones
The carboanion from acetophenone and propiophenone attacked the positively charged carbon of the 4(diphenylamino)benzaldehyde's carbonyl group. As a result, aldol condensation took place, yielding aldol compounds. The final products were formed by removing the hydroxyl group and forming a double bond (crotonic condensation). Alkaline catalyst was used, and the reactions were carried out at temperatures below 25 °C to prevent secondary reactions. Schemes 1 and 2 depict the synthetic approach to the targeted compounds. All of the triphenylamine chalcones that were synthesized came out as distinct shades of yellow powders. The yields for the compounds ranged from 30 to 92 percent (Table 1), which is a range of poor, moderate, and good yields when compared to chalcone compounds documented in the literature [16]. The triphenylamine chalcones were all synthesized in a single step, with no attempts of solid-state reactions (without the need of a solvent). The lowest yield was obtained with compound **2b,** which could be owing to the nature of the 2-bromo substituent on the B-ring of (propiophenone), which may prevent proper condensation of the reactants. The structures of the synthesized compounds were validated through extensive investigation of their FT-IR, GC–MS, and NMR spectra (see Additional file 1: Appendix attached) as well as available literature data; additionally, recrystallization and

Scheme 1 Synthesis of triphenylamine chalcone from substituted acetophenones (**1a**–**d**)

Scheme 2 Synthesis of triphenylamine chalcone from substituted propiophenones (**2a**–**d**)

Tukur *et al. Beni-Suef Univ J Basic Appl Sci*   (2022) 11:66

Page 7 of 11

Table 1 Physical data of the synthesized triphenylamine chalcones

Sample	B-ring	M.F	M.W (g)	Color	R_f	M.P range	Yield (%)
1a	4-Bromoacetophenone	$C_{27}H_{20}BrNO$	454	Deep yellow	0.67	145–147	70
1b	3-Nitroacetophenone	$C_{27}H_{20}N_2O_3$	420	Golden yellow	0.76	143–145	92
1c	4-Chloroacetophenone	$C_{27}H_{20}ClNO$	409	Yellow	0.69	137–139	57
1d	4-Fluoroacetophenone	$C_{27}H_{20}FNO$	393	Lemon green	0.83	136–138	60
2a	4-Hydroxypropiophenone	$C_{29}H_{25}NO_2$	419	Pale yellow	0.72	146–148	55
2b	2-Bromopropiophenone	$C_{29}H_{24}BrNO$	482	Brownish yellow	0.45	147–148	30
2c	4-methoxypropiophenone	$C_{31}H_{27}NO_2$	433	Orange yellow	0.75	142–144	52
2d	4-Flouropropiophenone	$C_{29}H_{24}FNO$	421	Cotton brown	0.64	146–148	54

M.F: molecular formula, M.W: molecular weight, M.P: melting point, R_f: retention factor

Table 2 Zone of inhibition (mm)

Test organisms	Triphenylamine chalcones									
	1a	1b	1c	1d	2a	2b	2c	2d	Cip	Flu
E. coli	14	16	15	20	13	18	19	16	30	–
P. aeruginosa	15	18	18	18	16	18	20	19	40	–
S. typhi	16	14	17	16	16	13	15	18	26	–
S. aureus	13	15	14	18	13	13	15	15	28	–
B. subtilis	16	17	20	17	18	20	20	18	25	–
MRSA	14	16	19	15	16	17	16	19	30	–
C. albicans	17	13	20	13	16	20	20	18	–	20
A. niger	25	30	23	20	20	22	21	23	–	22

–: Not determined, Cip: ciprofloxacin, Flu: Fluconazole

Table 3 Minimum inhibitory concentrations (MIC) of the synthesized compounds (μg/ml)

Test organisms	Triphenylamine chalcones							
	1a	1b	1c	1d	2a	2b	2c	2d
E. coli	100	100	100	25	100	50	25	100
P. aeruginosa	100	50	50	50	100	25	25	25
S. typhi	100	100	50	100	100	100	100	50
S. aureus	100	100	100	50	100	100	100	100
B. subtilis	100	50	25	25	25	25	25	50
MRSA	100	50	25	50	100	50	50	25
C. albicans	50	25	25	50	50	25	25	50
A. niger	12.5	12.5	12.5	12.5	25	25	25	12.5

TLC were used to establish their purity. The characterization of produced triphenylamine chalcones is briefly appraised here;

The bands ranged from 1684 to 1686 cm^{-1} for C=O stretching, 2996 to 3037 cm^{-1} for aromatic C–H stretching, and 2914 to 2933 cm^{-1} for aliphatic C–H stretching in the FT-IR spectra of the synthesized triphenylamine chalcones. The FT-IR spectra of all the synthesized triphenylamine chalcones revealed a similar band at 1267–1286 cm^{-1} due to C–N bending from the amino group. In the FT-IR spectra of the synthesized chalcones, a band between 1580 and 1584 cm^{-1} was seen, which is attributable to C=C stretching of the chromophores, confirming the production of a new C=C and the formation of the intended products. Different bands were observed due to the presence of different substitutions in the B-rings of the chalcones, which correspond to the type of substituents present, as follows: **1a** showed

Table 4 Minimum bactericidal/fungicidal concentrations (MBC/MFC) of the synthesized compounds (µg/ml)

Test organisms	Triphenylamine chalcones							
	1a	1b	1c	1d	2a	2b	2c	2d
E. coli	–	–	–	50	–	100	100	–
P. aeruginosa	–	100	100	100	–	100	50	100
S. typhi	–	–	100	–	–	–	–	100
S. aureus	–	–	–	100	–	–	–	–
B. subtilis	–	100	100	50	100	50	50	100
MRSA	–	–	100	100	–	100	–	100
C. albicans	100	100	50	100	100	50	50	100
A. niger	50	50	50	50	50	50	50	50

–: No MBC/MFC

a band at 530 cm^{-1}, which corresponds to C–Br bending, **1b** showed a band at 1390 cm^{-1}, which is due to N=O bending, **1c** showed a band at 620 cm^{-1}, which is due to C–Cl bending. Due to C–F bending, **1d** showed a band at 1073 cm^{-1}, whereas **2a** showed a broadband with intensity at 3243 cm^{-1} due to C–OH in the B-ring.

Compounds **2b** and **2c** showed a band at 580 cm^{-1} owing to C–Br bending, 1320 cm^{-1} due to C–O bending of the methoxy moiety in the B-ring, and 1028 cm^{-1} due to C–F bending. While compound **2d** showed a band at 1028 cm^{-1} due to C–F bending. All of the bands detected in the FT-IR spectra of the synthesized chalcones agreed with the values given in the literature. Thus, (C=O; 1684 cm^{-1}, C=C; 1577 cm^{-1}, C=N; 1286 cm^{-1}, C–Br; 530 cm^{-1}, –OH; 3230 cm^{-1},= C–H; 3037 cm^{-1}) (C=O; 1684 cm^{-1}, C=C; 1577 cm^{-1}, C=N; 1286 cm^{-1}, C=N; 1286 cm^{-1}, C=N; 1286 cm^{-1}, C=N; 1286 cm^{-1} [31, 32]. The GC–MS spectra of the synthesized chalcones revealed that all of the compounds' m/z values are equal to their respective theoretical molecular weights, indicating that the products were formed.

The effect of different electron releasing groups bonded to the B-ring at different positions of the synthesized chalcones structures can be clearly seen in their ^{1}H-NMR spectra, which showed the expected specific signal peaks of the new olefinic bond and the effect of different electron donation groups bonded to the B-ring at different positions of the synthesized chalcones structures. Signal shape, chemical shifts and coupling constants can all be used to easily select these signal systems. The presence of doublets for α-C and β-C with coupling constants (*J*) ranging from 11.3 to 15.3 Hz revealed that, the conjugated chromophores α-H and β-H are trans (*E* configuration of the double bond). All synthesized triphenylamine chalcones were geometrically pure and entirely trans (*E*) isomers, as indicated by the higher coupling constant values [31].

The ^{1}H-NMR spectrum of **1a** revealed doublets with a chemical shift of 8.03–7.35 ppm and a *J* value of 12–15.3 Hz at the 2-H and 3-H positions, confirming the formation of a new C=C bond. H-3′ and H-6′ of the B-ring are both *ortho* to bromine and appear as a doublet with a chemical shift of 7.68 ppm and 7.34 ppm, respectively, while H-3′ and H-5′ are also *ortho* to bromine and appear as a doublet with a chemical shift of 7.43 ppm. Shift values of 8.13–7.97 ppm with a higher (*J*) value of 12.3–14.0 Hz at H-2 and H-3 in the ^{1}H-NMR spectrum of **1b** confirm the formation of a new C=C double bond and the target product. Because the protons in the B-ring of **1b** are not equivalent, chemical shift values of 8.75 ppm and 8.47 ppm were assigned to the protons *ortho* to the nitro substituent at 2′-H and 4′-H, respectively. These two protons are more deshielded due to the electronegativity of the nitrogen atom in the B-ring, and 2′-H appears as a singlet, while 4′-H appears as a doublet. Signal peaks at 8.02 ppm were ascribed to *meta* protons at 5′-H, which experience less electronegative influence of the nitro group, while chemical shift values at 8.26 ppm were assigned to 6-H′, which seem closer to the carbonyl carbon of the chalcone. The ^{1}H-NMR spectrum of **1c** revealed a doublets signal peak with a chemical shift of 8.51–7.68 ppm and a higher (*J*) value of 13–14 Hz, confirming the formation of a new unsaturated C=C bond. The ^{1}H-NMR spectrum of **2a** showed a singlet peak and a substantially deshielded chemical shift value of 9.8 ppm, confirming the presence of an OH group in the B-ring chalcone. Because of the nature of the position of substitution in the B-ring (2-bromo) of **2b**, which is *ortho* to the carbonyl carbon, the protons in the B-ring appear non-equivalent in the ^{1}H-NMR spectrum of **2a**, where 3′-H, which is *ortho* to the bromine, coupled with 4′-H and appear as doublet at a chemical shift of 7.42 ppm, while a shift at

Tukur *et al. Beni-Suef Univ J Basic Appl Sci*   (2022) 11:66

Page 9 of 11

7.94 ppm, which appears as doublet, was assigned to 6′-H which is *ortho* to the alpha carbon, and is more downfield due to the electronegativity of the carbonyl oxygen. Both 5′-H and 4′-H of **2b**, on the other hand, are non-equivalent and appear as triplet at 7.39 ppm and 7.32 ppm, respectively. The *ortho* (12,16,18,22-H), *meta* (H-13,15,19,21), and *para* (14,20-H) positions of the protons of the diphenyl rings connected to nitrogen of the amino group are all equivalent in respect to position of nitrogen, because there is no electron releasing or withdrawing group attached to any ring carbon. The ^{1}H-NMR spectra of all the propiophenone derived triphenylamine chalcones (**2a**–**d**) showed a chemical shift range of 0.85–0.90 ppm, which is due to a methyl group on C-11′ position, and each appear as a doublet due to the (n + 1) rule, while a shift between 3.70 and 3.81 ppm was also observed in (**2a**-d), which is due to a single proton (methine proton) on C-2, which showed a multiplicity of quartet, due to the 3 neighboring methyl protons on 11′-H (Chavran et al., 2019).

The ^{13}C-NMR spectra of the synthesized triphenylamine chalcones showed highly deshielded carbon resonance in the range of 190.29–190.64 ppm for the carbonyl carbon, the carbon resonance in the range of 115.9–119.9 ppm represent the α-C and 120.7–149.68 ppm represent the β-C of the conjugated chromophores. The ^{13}C-NMR spectrum of **2c** showed highly deshielded carbon resonance at 168.14 ppm which was assigned to C–F of the B-ring at C-4′, while shift at 165.20 was shown by ^{13}C-NMR spectrum of **2c** which confirm the C-OCH$_3$ of the B-ring at C-4′ position, and a signal at 162.92 ppm, as shown by the ^{13}C-NMR spectrum of **2a**, was assigned to (C–OH) of the B-ring at C-4′ [31]. Because the carbon atoms in **1b** are not equivalent in the B-ring, the signal at 149.29 ppm was attributed to C-3′, the carbon carrying the nitro substituent, which appears further downfield than the remaining carbon atoms in the B-ring. C-6′ carbon, which appears closer to the carbonyl carbon and will be further downfield than the remaining carbon atoms in the B-ring, was likewise assigned to the signal at 133.82 ppm of **1b**. C-5′, which is *meta* to the nitro substituent, has a chemical shift of 131.29 ppm in the carbon spectra of **1b**, while C-4′ and C-2′, which are *ortho* and non-equivalent, have chemical shifts of 129.73 and 123.29 ppm, respectively. The chemical shift range of all the derived propiophenone triphenylamine chalcones (**2a**-d) was 17.73–17.80 ppm, which is due to a methyl group on C-11′, while a shift between 46.46 and 48.06 ppm was also found due to the methine carbon on C-2. The carbon atoms of the diphenyl rings connected to the nitrogen of the amino group are *ortho* (C-12,16,18,22), *meta* (C-13,15,19,21), and para (C-14,20). The ^{13}C-NMR spectrum of compound **2c** showed a chemical shift value of 55.29 ppm at (C-12′), which is ascribed to the presence of methoxy carbon (O-CH$_3$) in the B-ring [31].

4.2 Biological results

The presence of a reactive, α,β-unsaturated keto functionality in chalcones was discovered to undergo conjugate addition with a nucleophilic group, leading to their antibacterial activity, which can vary depending on the type and position of substituents on the aromatic rings. [31]. The nature, number, and position of the substituent(s) on both benzene rings of the chalcone have shown a wide range of pharmacological activities. For example, pyrimidinyl substitution on chalcone has potent anti-tumor properties (Jin et al. 2013), quinolone substitution on chalcone has potent antimalarial activity and thiophenol substitution on chalcone has potent antibreast cancer properties. All of the synthesized triphenylamine chalcones were found to possess outstanding antimicrobial activity against the investigated microorganisms, with a considerable zone of inhibition compared to the conventional medicines utilized. Compound **1b** with a 3-Nitro substitution on the B-ring inhibited *Aspergillus niger* the most, with a 30 mm zone of inhibition. Compounds **1a**, **2d**, **1c**, **2b**, and **2c** with 4-bromo, 4-flouro, 4-chloro, 2-bromo, and 4-methoxy substitutions inhibited *Aspergillus niger* with a zones of inhibition of 25 mm, 23 mm, 22 mm, and 21 mm, respectively. Against *Bacillus subtilis*, *Candida albicans*, *Aspergillus niger* and *Pseudomonas aeruginosa* compounds **1c**, **1d**, **2a**, **2b**, and **2c** each demonstrated a 20-mm zone of inhibition. Compounds **1a**, **1b**, and **2a** containing 4-bromo, 3-nitro, and 4-hydroxy substituents, had the smallest zone of inhibition against *Staphylococcus aureus*, *Candida albicans* and *Escherichia coli.*

Compounds **1a**, **1b**, **1c**, and **1d** had a zone of inhibition (25 mm, 30 mm, and 23 mm) against *Aspergillus niger* that was greater than the standard drugs (fluconozole and ciprofloxacin) (Table 2). Minimum inhibitory concentrations, as well as minimum bactericidal and fungicidal concentrations, were examined for the compounds that demonstrated significant activity. Antifungal activity was enhanced by chalcones with halogen substituents such as bromine and chlorine [37].

The MIC data (Table 3) revealed that compounds **1a**, **1b**, **1c**, **1d**, and **2d** had the lowest MIC and inhibit *Aspergillus niger* growth at 12.5 µg/mL. *Candida albicans*, *Bacillus subtilis*, MRSA, *Escherichia coli*, *Pseudomonas aeruginosa* and *Aspergillus niger* are all inhibited by compounds **1b**, **1c**, **1d**, **2a**, **2b**, **2c**, and **2d** at 25 µg/mL. Compounds **1a**, **1b**, **1c**, **1d**, **2a**, **2b**, **2c**, and **2d** inhibited the growth of *Pseudomonas aeruginosa*, *Bacillus subtilis*, *Candida albicans*, MRSA, *Salmonella*

Tukur *et al. Beni-Suef Univ J Basic Appl Sci*   (2022) 11:66

Page 10 of 11

typhi, *Staphylococcus aureus*, and *Escherichia coli* at 50 μg/mL. At a concentration of 100 μg/mL, compounds **1a**, **1b**, **1c**, **1d**, **2a**, **2b**, **2c**, and **2d** inhibit the development of *Escherichia coli*, *Pseudomonas aeruginosa*, Salmonella typhi, *Staphylococcus aureus*, Bacillus subtilis, and MRSA.

MBC/MFC results revealed that at 50 μg/mL, compounds **1a**, **1b**, **1c**, **1d**, **2a**, **2b**, **2c**, and **2d** completely killed *Escherichia coli*, *Pseudomonas aeruginosa*, *Bacillus subtilis*, *Candida albicans*, and *Aspergillus niger*, whereas compounds **1a**, **1b**, **1c**, **1d**, **2a**, **2b**, **2c**, and **2d**, required a concentration of 100 μg/mL to totally kill *Pseudomonas aeruginosa*, *Escherichia coli*, *Salmonella typhi*, *Staphylococcus aureus*, *Bacillus subtilis*, MRSA and *Candida albicans*, as indicated in Table 4 3-[1-oxo-3-(2,4,5-trimethoxyphenyl)-2-propenyl] was synthesized by Prasad et al. which was tested at a concentration of 100 μg/mL, -2H-1-benzopyran-2-ones demonstrated substantial antibacterial action against *Bacillus subtilis*, *Bacillus pumilis*, and *Escherichia coli*. The role of electron-releasing substituents such as nitro, hydroxyl, and methoxyl groups in increasing activity was discovered in the study.

On the observed zone of inhibition, which spanned between (13–30 mm) as indicated in Table 2, the synthesized chalcones demonstrated varying degrees of antibacterial activity against the tested microorganisms. The activities of the synthesized chalcones (**1a**, **1c**, **1d**, **2a**, **2b**, **2c**, and **2d**) were found to be lower than those of the standard drugs (Ciprofloxacin and Fluconazole), though compound **1b** with a NO_2 substituent on the B-ring showed a higher zone of inhibition (30 mm) against *Aspergillus niger* than Fluconazole (22 mm).

At a concentration of 12.5 μg/mL, compounds with 4-bromo, 4-chloro, and 4-flouro substituents inhibited the growth of *Aspergillus niger*, according to the MIC results. The electronic effects of substituents on the B-ring have contributed to these properties, while **1b** with NO_2 substituent on the B-ring showed the best activity against tested fungal strains. The electronic effect of substituents on the ring-B in the compounds could explain the disparities in activity results. It has been reported that substituents on a compound's benzene ring have a negative inductive effect on its antimicrobial activity [33].

Karthikeyan et al. [30] used the Claisen–Schimdt condensation method to synthesize 3-aryl-1-(2,4-dichloro-5-fluorophenyl)-2-propen-1-one, which had antifungal activity against *Aspergillus niger*. Compound **1b** had the highest zone of inhibition of 30 mm against *Aspergillus niger*, as well as the lowest MIC of 12.5 μg/mL and MBC/MFC of 50 μg/mL against *Aspergillus niger*. As a result, **1b** had a higher antifungal potential.

5 Conclusion

Eight novel triphenylamine chalcones with different substitution patterns were successfully synthesized via the conventional Claisen–Schmidt condensation reaction in an alkaline medium. The percentage yield of the synthesized triphenylamine chalcones ranged from 30 to 92%. Thin layer chromatography (TLC) was used to monitor the progress and completion of the reaction. The synthesized triphenylamine chalcones were purified by recrystallization method from ethanol. The synthesis of the target chalcones involves a nucleophilic enolate attack on the electrophilic carbonyl carbon of 4-(diphenylamino)benzaldehyde resulting in the formation of a new carbon–carbon bond. The structures of the triphenylamine chalcones were successfully characterized and confirmed by FT-IR, GC–MS and NMR spectroscopic and spectrometric techniques. The antimicrobial investigation revealed that (*E*)-3-(4-(diphenylamino)phenyl)-1-(3′-nitrophenyl)prop-2-en-1-one (**1b**) showed highest ZOI (30 mm), lowest MIC (12.5 μg/mL) and MBC/MFC (50 μg/mL) on *Aspergillus niger.*

Supplementary Information

The online version contains supplementary material available at https://doi.org/10.1186/s43088-022-00246-8.

Additional file 1. Appendix.

Author contributions
AT carried out the synthesis, the antimicrobial studies and produces the manuscript. RG guide the synthesis review the manuscript. ORAI guide the synthesis of the novel chalcones. JDH guide the synthesis, antimicrobial studies and the review of the manuscript. All authors read and approved the final manuscript.

Availability of data and materials
Not applicable.

Declarations

Ethics approval and consent to participate
Not applicable.

Tukur *et al. Beni-Suef Univ J Basic Appl Sci* (2022) 11:66

Page 11 of 11

Consent for publication

Not applicable.

Competing interest

The authors declare no competing interests.

References

1. Agilandeshwari R, Meenatchi V, Meenakshisundaram SP (2016) Synthesis, growth, structure and characterisation of chalcone crystal: a novel organic NLO material. J Mol Struct 1118:356–366
2. Ahmadi S, Mardinia F, Azimi N, Qomi M, Balali E (2019) Prediction of chalcone derivative cytotoxicity activity against MCF-7 human breast cancer cell. J Mol Struct 11:305–311
3. Aljamali N, Daylee SH, Kadhium AJ (2020) Review on chemical biological fields of chalcone compounds. Forefront J Eng Technol 2(1):33–44
4. Alswah M, Bayoumi AH, Elgamal K, Elmorsy A, Ihmaid S, Ahmed HE (2017) Design, synthesis and cytoxic evaluation of novel chalcones derivativeion inhibitory effects: Bearing triazolo [4,3-a]-quinoxaline moities as potent anticancer agents with dual EGFR kinase and tubulin polymerization inhibitory effects. Molecules 23(48):1–16
5. Asima H, Sara M, Aamir HE, Ahmed A, Sharif MI, Abdullah MY (2019) Antimalarial, cytotoxicity and molecular docking studies of quinolinyl chalcones as potential anti-malarial agent. J Comput Aided Mol Des 33(7):677–688. https://doi.org/10.1007/s10822-019-00210-2
6. Avila-Villarreal G, Hernández-Abreu O, Hidalgo-Figueroa S, Navarrete-Vázquez G, Escalante-Erosa F, Pena-Rodríguez LM, Estrada-Soto S (2013) Antihypertensive and vasorelaxant effects of dihydrospinochalcone-A isolated from *Lonchocarpus xuul* Lundell by NO production: computational and ex vivo approaches. Phytomedicine 20(14):1241–1246
7. Bagyaraj E, Moorthi K, Aboobuckersithique M (2017) Synthesis of novel chalcones. ChemiXpress 10(1):1–10
8. Bonakdar AP, Vafaei F, Farokhpour M, Esfahani MN, Massah AR (2017) Synthesis and anticancer activity assay of novel chalcone-sulfonamide derivatives. Iran J Pharm Res 16(2):565–568
9. Bruton LL, Lazo JS, Parker KL (2007) The pharmaceutical basis of therapeutics, 11th edn. Mc Graw-Hill, New York
10. Chantalle M, Rencia S, Richard B, Lesetja L (2020) An update on development of small-molecule *Plasmodial kinase* inhibitors. Molecules 25(21):5182
11. Chao-Fan Lu, Sheng-Hui W, Xiao-Jing P, Ting Z, Hong-Li Li, Qing-Rong L, Qian-Yu L (2020) Synthesis and biological evaluation of amino chalcone derivatives as antiproliferative agents. Molecules 25(23):5530
12. Chavan BB, Gadekar AS, Mehta PP, Vawhal PK, Kolsure AK, Chabukswar., A. R. (2016) Synthesis and medicinal significance of chalcones—a review. Asian J Biomed Pharm Sci 6(56):01–07
13. Chen Q, Xu L, Liang C, Wang C, Peng R, Liu Z (2016) Photothermal therapy with immune-adjuvant nanoparticles together with checkpoint blockade for effective cancer immunotherapy. Nat Commun 7(1):13193. https://doi.org/10.1038/ncomms13193
14. Chunlin Z, Wen Z, Chunquan S, Wannian Z, Chengguo X, Zhenyuan M (2017) Chalcone: a privileged structure. Med Chem 117(12):7762–7810
15. Climent MJ, Corma A, Iborra S, Velty A (2018) Synthesis of chalcones: a review. J Mol Catal 2(21):474–500
16. Eddarir S, Cotelle N, Bakkour Y, Rolando C (2003) An efficient synthesis of chalcones based on the Suzuki reaction. Tetrahedron Lett 44:5359–5363
17. Efraín P, Ibarra-Arellano N, Prent-Peñaloza L, Morales-Bayuelo A, Henao J, Galdámez A, Gutiérrez M (2019) Ultrasound-assisted synthesis of novel chalcone, heterochalcone and bis-chalcone derivatives and the evaluation of their antioxidant properties and as acetylcholinesterase inhibitors. Bioorg Chem 90:103034
18. ElMonaem HS, Abdel-Aziz NI, Morsi MA, Badria FA, ElSenduny F, El-Ashmawy MB, Moustafa MA (2018) Synthesis, in vitro antiproliferative evaluation and molecular docking of new tetrazole-chalcone and tetrazole-pyrazoline hybrids. J Appl Pharm Sci 8(5):075–087
19. Farooq S, Ngaini Z (2019) Recent synthetic methodologies for chalcone synthesis. Curr Organocatal 6:184–192
20. Frazier Z (2020) Screening a library of chalcone derivatives for antibacterial properties *via* Kirby Bauer disk diffusion. Undergraduate Theses, 44
21. Funiss BS, Hannford AJ, Smith PWG, Tatchell AR (2018) Vogel's textbook of practical organic chemistry, 5th edn., pp 1032–1035
22. Hayreddin G, Meliha B, Gürdere A, Dinçer O, Özbek Ü, Koçyiğit P, Taslimi B, Tüzün Y, Budak M (2021) Synthesis, molecular docking, and biological activities of new cyanopyridine derivatives containing phenylurea. Arch Pharm 354(4):2000334
23. Li H, Huang J, Chen L, Liu X, Chen T, Zhu J, Lu W, Shen X, Li J, Hilgenfeld R, Jiang H (2019) Identification of novel falcipain-2 inhibitors as potential antimalarial agents through structure-based virtual screening. J Med Chem 52(15):4936–4940
24. Hongtian Z, Lei T, Chenghong Z, Baochu W, Pingrong Y, Dian H, Lifang Z, Yang Z (2019) Synthesis of chalcone derivatives: inducing apoptosis of HepG2 cells *via* regulating reactive oxygen species and mitochondrial pathway. Front Pharmacol. https://doi.org/10.3389/fphar.2019.01341
25. Hua L, Chuanlong G, Shuju G, Wang D (2019) Design and synthesis of a fluorescent probe with a large stokes shift for detecting thiophenols and its application in water samples and living cells. Molecules 24(2):375
26. Jae-Chul J, Yongnam L, Dongguk M, Mankil J, Seikwan O (2018) Practical synthesis of chalcone derivatives and their biological activities. Molecules 22(11):1872
27. Jaiswal P, Dharam P, Himangini B, Uma A (2018) Chalcone and their heterocyclic analogue. J Chem Pharm Res 10(4):160–173
28. Ji X, Lu Y, Tian H, Meng X, Wei M, Cho WC (2019) Chemoresistance mechanisms of breast cancer and their countermeasures. Biomed Pharmacother 57:315–320
29. Karou D, Savadogo A, Canini A, Yameogo S, Montesano C, Simpore J, Colizzi V, Traore AS (2006) Antibacterial activity of alkaloids from Sida acuta. Afr J Biotechnol 5(2):195–200
30. Karthikeyan C, Moorthy NS, Ramasamy S, Vanam U, Manivannan E, Karunagaran D, Trivedi P (2015) Advances in chalcones with anticancer activities. Recent Patents 10:97–115
31. Kayode LA, Isaac AB, Adebayo OO (2019) Synthesis, characterization and antifungal study of five new derivatives of *E*-1-(2-Hydroxyphenyl)chalcone. Chem Afr 2:1–14
32. Kumar KG, Tripathi V, Knyar P, Gupta LP, Trivedi R, Bid H, Chattopadhyay N (2014) Design and synthesis and characterization of 1,3-biarylsulfanyl chalcone. Bioorg Med Chem 19:409–419
33. Narain Y, Jhaumeer-Laulloo S, Bhowon MG (2010) Structure– activity relationship of Schif base derivatives. Int J Biol Chem Sci 4(1):69–74
34. Pradip S, Khushboo M, Anand C, Devanshi G, Sudha S, Sweta K, Meena K (2016) Activity of newly synthesized chalcone derivatives against H1N1 virus supported by molecular docking and membrane interaction studies. J Antivirous Antiretrovir 8(2):79–89
35. Rücker H, Al-Rifai N, Rascle A, Gottfried E, Brodziak-Jarosz L, Gerhäuser C, Amslinger S (2015) Enhancing anti-inflammatory activity of chalcones by tuning the Michael acceptor site. Biomol Chem 13(10):3040–3047
36. Sangeetha M, Reichal CR, Thirumoorthy N (2017) Synthesis and biological evaluation of some novel heterocyclic chalcone derivatives. World J Pharm Life Sci 3(6):263–267
37. Shaik KY, Vidya SD, Afzal BS (2015) Chemical and biological potentials of chalcones: a review. Org Med Chem 1(1):53
38. Shukla P, Satyanarayana M, Verma PC, Tiwari J, Dwivedi AP, Srivastava R, Pratap R (2017) Chalcone-based aryloxypropanolamine as a potential antidiabetic and antidyslipidaemic agent. Curric Sci 12(8):1675–1689
39. Tukur AR, Habila JD, Ayo RGO, Lyun ORA (2022) Synthesis, reactions and pharmacological applications of chalcones and their derivatives—a mini review. J Chem Rev 4(2):100–119
40. Xu Z, Zhao S, Lv Z, Feng L, Wang Y, Zhang F, Deng J (2019) Benzofuran derivatives and their anti-turbacular and anti-bacterial activities. Eur J Med Chem 162:266–276

Publisher's Note